LETTER

doi:10.1038/nature12467

Evolutionary implications of a third lymphocyte lineage in lampreys

Masayuki Hirano[1], Peng Guo[1]†, Nathanael McCurley[1], Michael Schorpp[2], Sabyasachi Das[1], Thomas Boehm[2] & Max D. Cooper[1]

Jawed vertebrates (gnathostomes) and jawless vertebrates (cyclostomes) have different adaptive immune systems[1,2]. Gnathostomes use T- and B-cell antigen receptors belonging to the immunoglobulin superfamily[3,4]. Cyclostomes, the lampreys and hagfish, instead use leucine-rich repeat proteins to construct variable lymphocyte receptors (VLRs), two types of which, VLRA and VLRB, are reciprocally expressed by lymphocytes resembling gnathostome T and B cells[5–7]. Here we define another lineage of T-cell-like lymphocytes that express the recently identified VLRC receptors[8,9]. Both VLRC$^+$ and VLRA$^+$ lymphocytes express orthologues of genes that gnathostome γδ and αβ T cells use for their differentiation, undergo *VLRC* and *VLRA* assembly and repertoire diversification in the 'thymoid' gill region, and express their VLRs solely as cell-surface proteins. Our findings suggest that the genetic programmes for two primordial T-cell lineages and a prototypic B-cell lineage were already present in the last common vertebrate ancestor approximately 500 million years ago. We propose that functional specialization of distinct T-cell-like lineages was an ancient feature of a primordial immune system.

The invariant stalk region of the sea lamprey VLRC shares approximately 20% sequence identity with the invariant VLRA and VLRB stalk regions, and distinguishing VLRC sequences are also present in the amino-terminal and carboxy-terminal leucine-rich repeat regions[8,9]. Four mouse monoclonal antibodies specific for the VLRC protein were produced, all of which identified a third lymphocyte population in lampreys that did not express VLRA or VLRB (Fig. 1a and Supplementary Fig. 1). VLRC$^+$ lymphocytes were more numerous than VLRA$^+$ lymphocytes in the principal lymphoid tissues of lamprey larvae (blood, kidneys, typhlosole and gill region) and they constituted the majority of lymphocytes in typhlosole and gills, whereas VLRB$^+$ lymphocytes predominated in blood and kidneys (Fig. 1a).

Immunofluorescence analysis of tissue sections indicated a similar distribution pattern for VLRA$^+$ and VLRC$^+$ lymphocytes in the typhlosole (Fig. 1b), kidneys (Fig. 1c), gills (Fig. 1d) and hypopharyngeal fold (Fig. 1e). Both cell types were round or oval in shape within blood vessels and interstitial spaces of the kidneys and typhlosole, but were dendritic in shape in the gill and intestinal epithelium (see inset in Fig. 1d) where the VLRC$^+$ cells were more numerous (VLRC/VLRA ratio of approximately 1.7/1) (Fig. 1b, f) and VLRB$^+$ cells were infrequent. VLRC$^+$ cells with inter-digitating morphology were the dominant lymphocyte type in the epidermal region of the skin (VLRC/VLRA ratio of 8/1) (Fig. 1f, g), a site in which VLRB$^+$ cells were rarely observed. The predominance of VLRC$^+$ cells in the epidermis is reminiscent of the dendritic epidermal T cells in mice, which express the same canonical γδ T-cell receptor (TCR)[10]. When *VLRC* sequences for the VLRC$^+$ cells in different tissues were compared, repetitive *VLRC* sequences were abundant in the skin, but rare in kidney and blood samples (Fig. 1h). We found several examples of identical or almost identical *VLRC* sequences in skin samples from different animals (Supplementary Fig. 2), suggesting that the *VLRC* repertoire in the skin is less diverse and more stereotypic than elsewhere. Importantly,

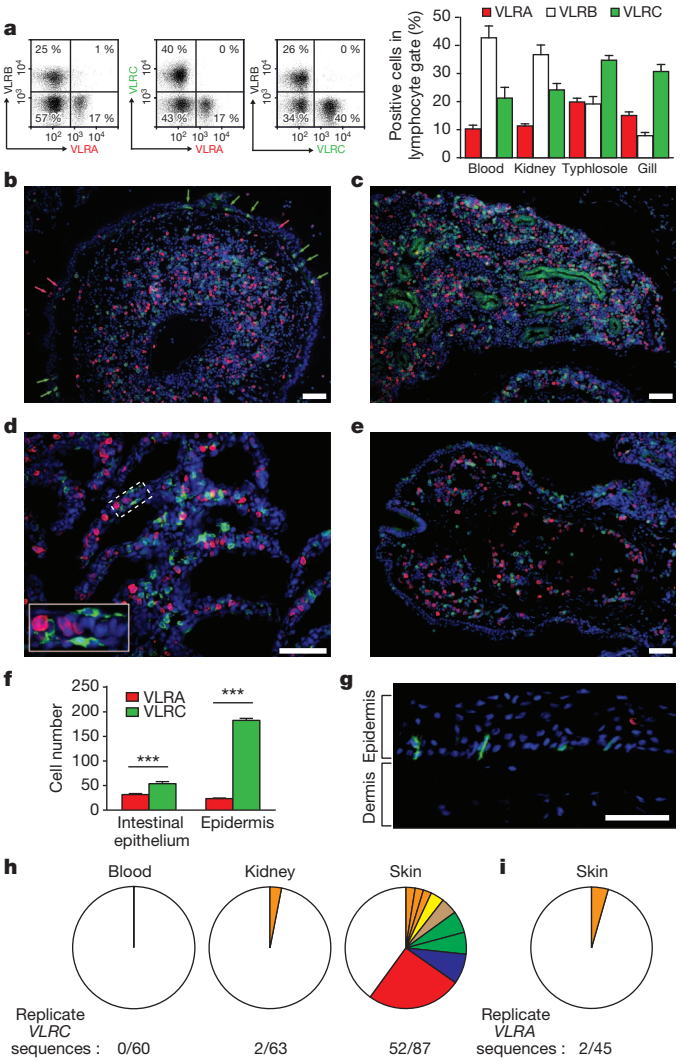

Figure 1 | Tissue distribution of VLRA$^+$, VLRB$^+$ and VLRC$^+$ lymphocytes. **a**, Flow cytometric analysis of lymphocyte-gated cells stained with monoclonal antibodies specific for VLRA (R110), VLRB (4C4) and VLRC (3A5) (left). Lymphocyte population in lamprey larvae (right); $n = 11$. **b–g**, Immunofluorescence staining of VLRC$^+$ (green) and VLRA$^+$ (red) lymphocytes in larval tissue sections, and DAPI counterstaining of nuclei (blue); scale bars, 50 μm (**b–e**, **g**). Shown are typhlosole surrounded by intestinal epithelium (intraepithelial lymphocytes) (**b**, arrows), kidneys (**c**), gill filaments (**d**; inset is a magnification of the area indicated by the dashed box), hypopharyngeal fold (**e**), skin (**g**). Lymphocyte distribution in the intestinal epithelium and skin epidermis is shown in **f**; $n = 5$ larvae. ***$P < 0.0001$; error bars, s.e.m. **h**, Frequency of replicate *VLRC* sequences in indicated tissues from two larvae; replicate VLRC sequences were not shared by different tissues. **i**, Frequency of *VLRA* replicates. The numbers of clonal replicates are colour-coded: red, 22; blue, 7; green, 5; pale orange, 4; yellow, 3; orange, 2.

[1]Emory Vaccine Center and Department of Pathology and Laboratory Medicine, Emory University, 1462 Clifton Road North-East, Atlanta, Georgia 30322, USA. [2]Department of Developmental Immunology, Max Planck Institute of Immunobiology and Epigenetics, Stuebeweg 51, Freiburg D-79108, Germany. †Present address: Novo Nordisk Research Centre China, 20 Life Science Park Road, Beijing 102206, China.

restricted diversity was not observed for *VLRA* sequences isolated from the same skin samples (Fig. 1i).

Antigen-binding VLRB$^+$ lymphocytes respond to immunization with proliferation and differentiation into plasma cells that secrete VLRB antibodies[11,12]. VLRA$^+$ lymphocytes also proliferate in response to immunization, but fail to bind unmodified immunogens, either before or after immunization, and do not differentiate into VLRA-secreting cells[5]. Proliferative responses to *Bacillus anthracis* exosporium were also observed for VLRC$^+$ lymphocytes (Fig. 2a and Supplementary Fig. 3a). The VLRC$^+$ lymphocytes also responded to the plant mitogen phytohaemagglutinin (PHA) with vigorous proliferation (Fig. 2b) and increased cell numbers (Fig. 2c and Supplementary Fig. 3b) and the activated VLRC$^+$ cells resembled activated VLRA$^+$ cells, in that they were large lymphoblasts with limited endoplasmic reticulum (Supplementary Fig. 3c). Nevertheless, plasma samples from naive or PHA-stimulated lampreys were devoid of VLRC protein (Fig. 2d) and *VLRC* transfectants did not secrete the VLRC protein (Supplementary Fig. 4).

Gene-expression profiles were compared for VLRA$^+$, VLRB$^+$, VLRC$^+$ and triple-negative populations of cells with lymphocyte light-scattering characteristics by examining the expression levels of a selected panel of orthologous genes. Discriminating profiles that were observed for the different populations included genes for transcription factors, cytokines or chemokines and their receptors, integrins, Toll-like receptors (TLRs), and various signalling molecules (Fig. 3a and Supplementary Tables 1 and 2). This analysis confirmed the clear dichotomy of the VLRB$^+$ B-like and the VLRA$^+$ T-cell-like lymphocytes. Although the transcriptional profiles were more similar for VLRA$^+$ and VLRC$^+$ cells, they differed in certain aspects; genes were expressed preferentially by VLRA$^+$ lymphocytes for the T-cell factor 1 (TCF1, also known as transcription factor 7), a key transcription factor for αβ T-cell lineage determination, and CTLA4, an important regulatory co-receptor for mammalian T cells. Conversely, VLRC$^+$ lymphocytes preferentially expressed the SRY-box containing gene 13 (SOX13) encoding a fate-determining transcription factor used for γδ T-cell lineage commitment[13,14], an integrin αL (ITGAL) orthologue of one component of the heterodimeric lymphocyte function associated antigen 1 (LFA1), and integrins

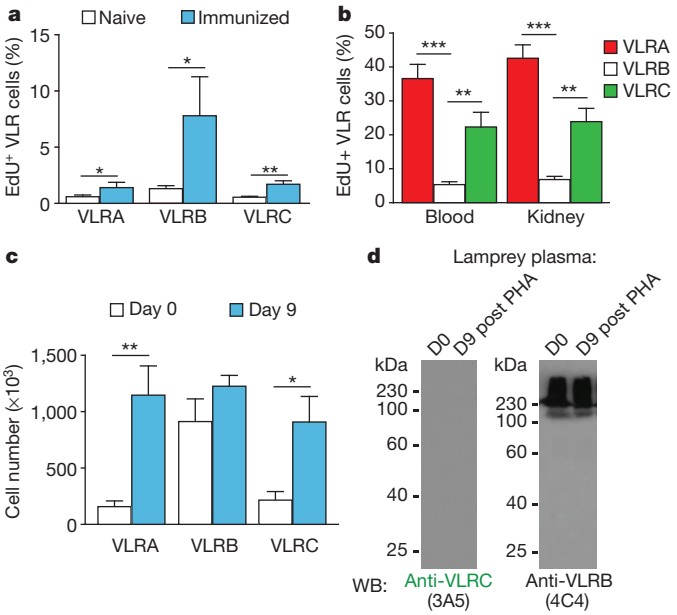

Figure 2 | Antigen and mitogen responses. **a**, Lymphocyte proliferation in typhlosole before ($n = 6$) and 28 days after ($n = 3$) *B. anthracis* exosporium immunization measured by EdU (5-ethynyl-2′-deoxyuridine) incorporation. **b**, Lymphocyte proliferation 9 days after PHA stimulation ($n = 7$). **c**, Lymphocyte numbers in blood after PHA stimulation ($n = 7$). **d**, Western blot (WB) analysis of plasma before (day 0 (D0)) and 9 days after (D9) PHA stimulation. kDa, kilodaltons. $^*P < 0.05$, $^{**}P < 0.01$, $^{***}P < 0.001$; error bars, s.e.m.

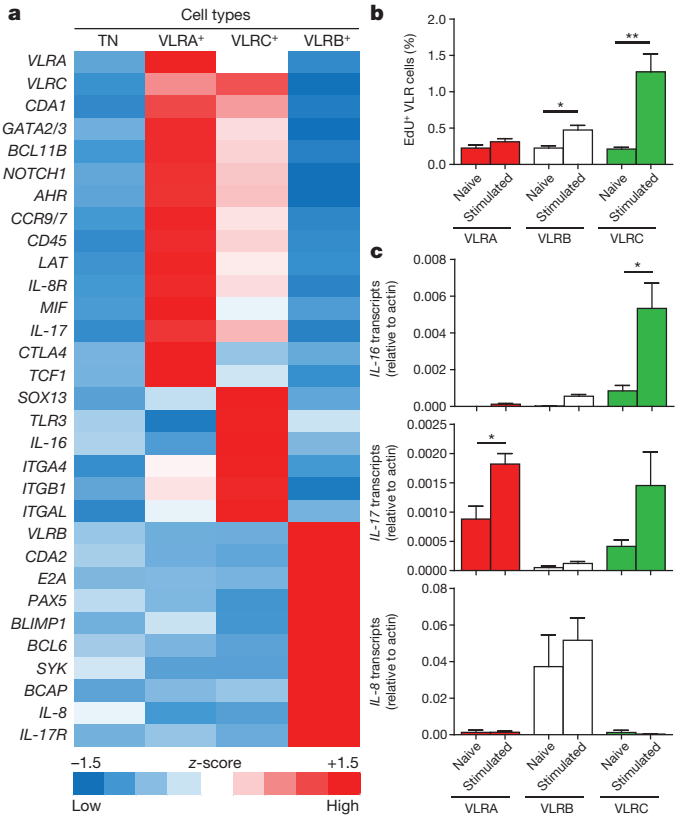

Figure 3 | Gene-expression profiles of VLRA$^+$, VLRB$^+$ and VLRC$^+$ lymphocytes and their poly(I:C) responses. **a**, Relative transcript levels of the indicated genes were measured by quantitative PCR for purified VLRA$^+$, VLRB$^+$, VLRC$^+$ and triple negative (TN) lymphocyte populations and compiled into a heat map ($n = 5$). **b**, Proliferative responses to *in vivo* poly(I:C) stimulation, measured by EdU incorporation ($n = 3$). **c–e**, Cytokine expression of purified blood lymphocytes before and 9 days after poly(I:C) treatment of lamprey larvae measured by quantitative PCR ($n = 3$): **c**, *IL-16*, **d**, *IL-17* and **e**, *IL-8*. $^*P < 0.05$, $^{**}P < 0.01$; error bars, s.e.m.

α4 and β1 (ITGA4 and ITGB1) orthologues of the two components of very late antigen 4 (VLA4), the expression of which was correlated with adherence of human γδ T cells to epithelial cells[15], TLR3 (ref. 16) and interleukin-16 (IL-16), a modulator of T-cell activation[17].

The functional implication of the preferential *TLR3* expression by lamprey VLRC$^+$ lymphocytes was examined by comparing the VLRA$^+$, VLRB$^+$ and VLRC$^+$ lymphocyte responses to poly(I:C), a structural mimic of double-stranded RNA. This analysis revealed a preferential proliferative response by VLRC$^+$ lymphocytes (Fig. 3b); VLRB$^+$ lymphocytes also responded to a lesser extent. Poly(I:C) stimulation also enhanced the expression of *IL-16* transcripts by VLRC$^+$ cells, while having only a slight effect on *IL-17* expression by the VLRA$^+$ and VLRB$^+$ cells and no effect on *IL-8* expression by VLRB$^+$ cells (Fig. 3c). These results suggest that TLR3 expression by VLRC$^+$ lymphocytes could potentially facilitate their participation in responding to infection with RNA viruses, akin to the modulation of γδ T cell responses by TLRs in mammals[18].

To determine whether *VLRC* assembly accompanies *VLRA* assembly in the thymus-equivalent region at the tips of the gill filaments[19], we compared DNA samples obtained by laser capture micro-dissection of cells from the 'thymoid' region, which is characterized by ongoing CDA1 expression, and from blood where CDA1 expression is undetectable (Fig. 4a, b). Functional and non-functional *VLRC* assemblies were observed in both locations, although non-functional *VLRC* assemblies were present in higher frequency in the 'thymoid' region (14 non-functional out of 61 total distinct *VLRC* assemblies) than in blood (7 non-functional out of 100 total *VLRC* assemblies). Moreover, most of the non-functional

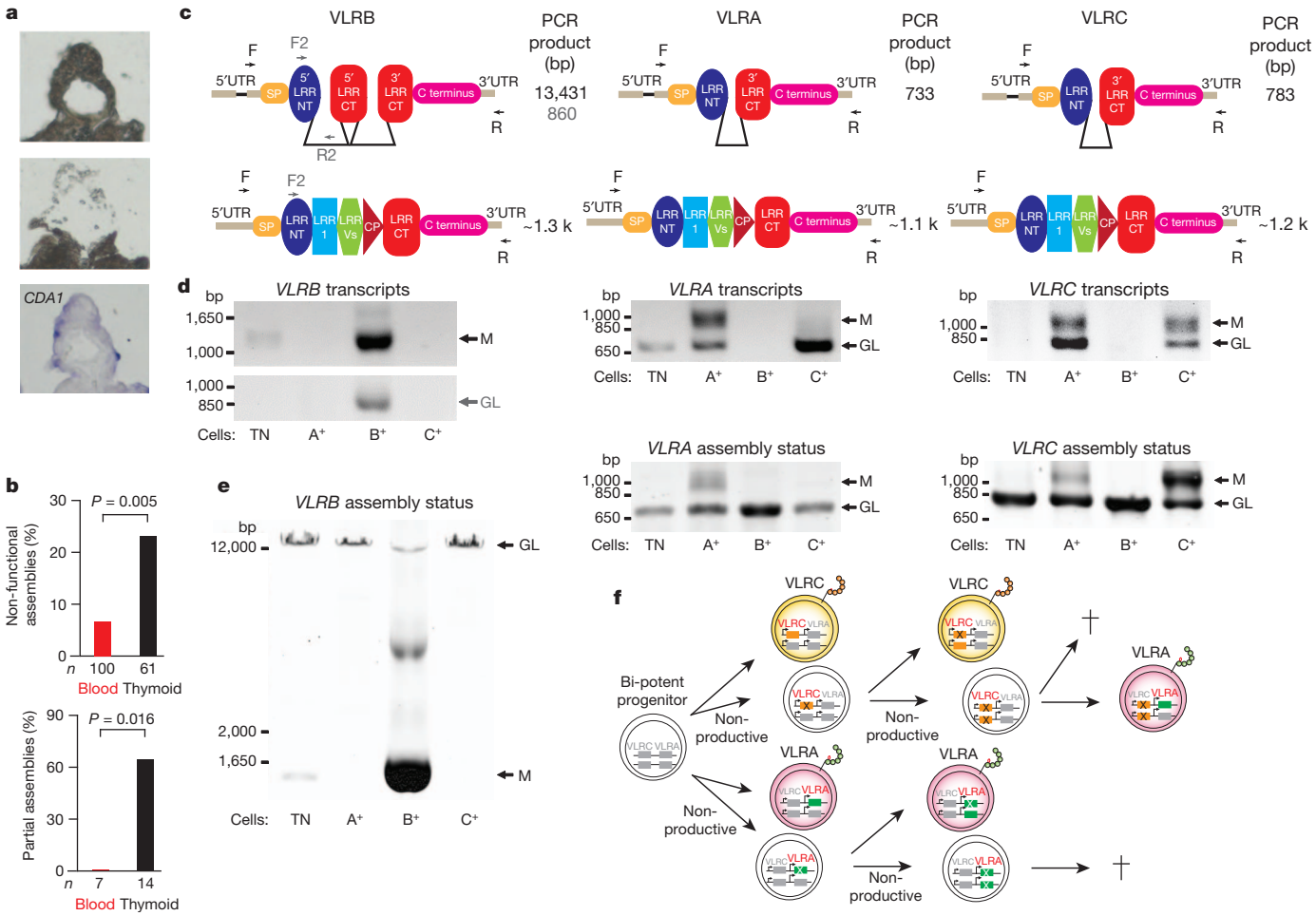

Figure 4 | Analysis of *VLRC*, *VLRA* and *VLRB* transcription and assembly. **a**, Thymoid procurement site before (top) and after (middle) laser-capture micro-dissection; *CDA1*-expressing cells (blue) were detected by RNA *in situ* hybridization in an adjacent section (bottom). **b**, Proportion of non-productive sequences among assembled *VLRC* genes (top) and partially assembled genes among non-productive *VLRC* sequences (bottom). **c**, Schematic of *VLR* genes before (top) and after (bottom) assembly. Forward (F) and reverse (R) primer locations and predicted PCR product sizes are indicated. The F2 and R2 primer pair (grey) was used to amplify *VLRB* transcripts. **d**, Total RNA extracted from purified lymphocyte populations was amplified by RT–PCR (PCR with reverse transcription). bp, base pairs; GL, germline transcripts; M, transcripts of assembled *VLR* genes. **e**, Assembly of *VLRB*, *VLRA* and *VLRC* genes identified by PCR of genomic DNA. **f**, Schematic model of VLRA and VLRC assembly during the development of bi-potent precursor cells in the 'thymoid'. Orange bars indicate *VLRC* assembly, green bars indicate *VLRA* assembly (solid coloured bars, productive assembly; bars with a cross, non-productive assembly). Green and orange chains represent leucine-rich repeat modules of VLRA and VLRC, respectively. Red text represents genes that are assembled. Grey text represents genes that are not assembled. Dagger symbols represent cell death.

VLRC sequences in cells within the 'thymoid' region consisted of incomplete intermediate-stage assemblies (9 out of 14), whereas incomplete *VLRC* assemblies were not found among the non-functional *VLRC* assemblies in blood (0 out of 7).

Transcription profiles for the *VLR* loci and their assembly status were examined in VLRA$^+$, VLRB$^+$, VLRC$^+$ and triple-negative lymphocyte populations purified by fluorescence-activated cell sorting from pooled cell suspensions derived from the blood, gills, kidneys, typhlosole and skin of lamprey larvae. Each sample was divided into two aliquots, which were used for genomic DNA and RNA transcript analysis. The polymerase chain reaction (PCR) products for the assembled or mature *VLRA* and *VLRC* genes were larger than those for the germline genes (see Fig. 4c), thus allowing their discrimination, purification and sequence analysis. Both germline and assembled *VLRB* genes were transcribed in VLRB$^+$ cells, whose *VLRA* and *VLRC* genes were transcriptionally silent (Fig. 4d). Conversely, *VLRB* transcription was not detected in VLRA$^+$ or VLRC$^+$ cells. However, both *VLRA* and *VLRC* loci were transcriptionally active in VLRA$^+$ and VLRC$^+$ lymphocytes. Hence, the expression of *VLRA* and *VLRC* genes was not lineage-specific, in contrast to the distinct cell surface phenotypes of VLRA$^+$ and VLRC$^+$ lymphocytes.

Consistent with previous studies indicating that mono-allelic assembly is the rule for VLRA$^+$ lymphocytes[5], we observed an approximately 50/50 ratio of assembled versus non-assembled *VLRA* genes in VLRA$^+$ cells (Fig. 4e) and sequence analysis indicated that 94% (99 out of 105) of the *VLRA* assemblies in VLRA$^+$ cells were functional. *VLRC* assemblies were also detected in the VLRA$^+$ cells (Fig. 4e), but 79% (46 out of 58) of these were non-productive assemblies. The *VLRA* and *VLRC* assembly status was more complex for the VLRC$^+$ cells, as indicated by the 65/35 ratio of assembled versus non-assembled *VLRC* genes (Fig. 4d, e). The predominance of assembled gene products in VLRC$^+$ cells suggested the presence of bi-allelic *VLRC* assemblies in a fraction of these cells, and approximately 15% (20 out of 132) of the *VLRC* assemblies in VLRC$^+$ cells were non-productive. Conversely, *VLRA* assemblies were rarely detected in VLRC$^+$ cells, and almost all of these were non-productive (54 out of 55). Most non-functional *VLRA* and *VLRC* sequences contained frame-shift mutations (Supplementary Fig. 5), and stop-codon mutations were less common. These composite results suggest a differentiation model in which bi-potential precursor cells begin to undergo *VLRC* or *VLRA* assembly in the 'thymoid', and the assembly process may proceed to involve both alleles and even both loci to achieve a

productive *VLRC* or *VLRA* assembly in order to survive as receptor positive cells (Fig. 4f).

The present studies demonstrate that lampreys possess two T-cell-like lineages that exhibit mutually exclusive expression of their VLRA and VLRC surface proteins and have overlapping but distinct gene expression profiles. Their currently defined characteristics are reminiscent of the two principal T-cell lineages in jawed vertebrates. In several aspects, the gene-expression profiles of $VLRA^+$ and $VLRC^+$ cells resemble those of mammalian $TCR\alpha\beta^+$ and $TCR\gamma\delta^+$ T cells, although these lymphocyte lineages clearly cannot be considered to be precise equivalents. In addition to the convergent evolution of entirely different types of recognition receptors, other divergent modifications have almost certainly occurred during the approximately 500 million years of evolution since jawless and jawed vertebrates last shared a common ancestor. It will thus be particularly important to establish the degree of functional similarity between these T-cell lineages in future studies.

Our present results firmly establish the 'thymoid' region of the gill tips as the site of *VLRA* and *VLRC* assembly, and indicate that the epithelial microenvironment of this primary lymphoid organ provides the necessary signals to support the development of the two T-cell-like lineages of lymphocytes identified here. The thymoid thus parallels the jawed vertebrate thymus in its support of both $TCR\alpha\beta^+$ and $TCR\gamma\delta^+$ T-cell lineage differentiation. Incomplete intermediate *VLRC* assemblies were found only in 'thymoid' cells, as shown previously for *VLRA* assemblies[19]. These findings also indicate that *VLRA* and *VLRC* gene assemblies are both associated with *CDA1* expression in the 'thymoid' region of the gills, whereas *CDA2* expression and *VLRB* assembly occur in the haematopoietic typhosole and kidney tissues in lamprey larvae[19]. Our analysis of *VLRA* and *VLRC* expression and assembly in 'thymoid' cells and in $VLRA^+$ and $VLRC^+$ lymphocytes throughout the body suggests that bi-potent lymphoid progenitors undergo a complex pattern of *VLRC* versus *VLRA* assembly in which *VLRC* assembly precedes *VLRA* assembly in the 'thymoid'.

The findings here reveal functional similarities and differences between the three lymphocyte lineages of lamprey larvae. Unlike $VLRB^+$ cells, the $VLRC^+$ and $VLRA^+$ lymphocytes preferentially populate the pharyngeal and intestinal epithelium. Both thymoid-derived lymphocyte types can be activated by antigen stimulation or by the polyclonal mitogen PHA to undergo lymphoblastoid transformation and cell division, but do not differentiate into VLR-secreting cells, a chief difference to $VLRB^+$ cells. Notably, the $VLRC^+$ cells constitute the predominant lymphocyte population in the lamprey epidermis, and the repertoire of $VLRC^+$ cells derived from skin samples is restricted relative to that for $VLRC^+$ cells in other tissue sites. These interesting findings, which bring to mind the canonical γδ TCR expressed by dendritic epithelial T cells in mice[10] and the antigen-specific αβ T cells that patrol the skin of mice after herpes virus infection[20], emphasize the need to elucidate the mode of antigen recognition by the VLRC- and VLRA-bearing cells.

In conjunction with the previously documented dichotomy of B- and T-cell-like lymphocytes in lamprey, these results offer fresh insight into the evolution of the alternative adaptive immune systems of jawless and jawed vertebrates. Representative species of the two vertebrate lineages use different sets of genes and different combinatorial mechanisms to construct diverse antigen recognition receptors, but they show the same basic principle of lymphocyte differentiation along two distinct T-cell-like lineages and one B-cell-like lineage. These composite findings suggest that the basic genetic program regulating the developmental pathways of the three lymphocyte lineages must have already existed in a common ancestor for all vertebrates (Supplementary Fig. 6) and this constitutes a fundamental organizing principle for lymphocyte-based adaptive immune systems.

METHODS SUMMARY

Two outbred species of lamprey larvae (*Petromyzon marinus* and *Lampetra planeri*) were captured in the wild and housed in sand-lined aquaria. Methods were as described previously[5,19], except as noted below. *VLRC* complementary DNA constructs[9] were cloned into a fusion vector to produce chimaeric proteins of the VLRC antigen-binding domain and stalk region fused to the constant region of human immunoglobulin-G1 (IgG1). Lymphocytes from mice immunized with the chimaeric proteins were used for hybridoma production, and supernatants were screened for antibody reactivity against recombinant VLRC. Monoclonal antibodies specific for VLRC were used together with anti-VLRA and -VLRB antibodies for characterizing and purifying VLR-expressing cells. Target gene sequences derived from the lamprey genome database[21] were used for quantitative real-time PCR analysis of genes and transcripts of the purified lymphocyte populations.

Full Methods and any associated references are available in the online version of the paper.

Received 22 March; accepted 15 July 2013.
Published online 11 August 2013.

1. Flajnik, M. F. & Kasahara, M. Origin and evolution of the adaptive immune system: genetic events and selective pressures. *Nature Rev. Genet.* **11,** 47–59 (2010).
2. Litman, G. W., Rast, J. P. & Fugmann, S. D. The origins of vertebrate adaptive immunity. *Nature Rev. Immunol.* **10,** 543–553 (2010).
3. Tonegawa, S. Somatic generation of antibody diversity. *Nature* **302,** 575–581 (1983).
4. Davis, M. M. & Bjorkman, P. J. T-cell antigen receptor genes and T-cell recognition. *Nature* **334,** 395–402 (1988).
5. Guo, P. *et al.* Dual nature of the adaptive immune system in lampreys. *Nature* **459,** 796–801 (2009).
6. Hirano, M., Das, S., Guo, P. & Cooper, M. D. The evolution of adaptive immunity in vertebrates. *Adv. Immunol.* **109,** 125–157 (2011).
7. Boehm, T. *et al.* VLR-based adaptive immunity. *Annu. Rev. Immunol.* **30,** 203–220 (2012).
8. Kasamatsu, J. *et al.* Identification of a third variable lymphocyte receptor in the lamprey. *Proc. Natl Acad. Sci. USA* **107,** 14304–14308 (2010).
9. Das, S. *et al.* Organization of lamprey variable lymphocyte receptor C locus and repertoire development. *Proc. Natl Acad. Sci. USA* **110,** 6043–6048 (2013).
10. Vantourout, P. & Hayday, A. Six-of-the-best: unique contributions of gammadelta T cells to immunology. *Nature Rev. Immunol.* **13,** 88–100 (2013).
11. Alder, M. N. *et al.* Antibody responses of variable lymphocyte receptors in the lamprey. *Nature Immunol.* **9,** 319–327 (2008).
12. Herrin, B. R. *et al.* Structure and specificity of lamprey monoclonal antibodies. *Proc. Natl Acad. Sci. USA* **105,** 2040–2045 (2008).
13. Melichar, H. J. *et al.* Regulation of γδ versus αβ T lymphocyte differentiation by the transcription factor SOX13. *Science* **315,** 230–233 (2007).
14. Rothenberg, E. V., Moore, J. E. & Yui, M. A. Launching the T-cell-lineage developmental programme. *Nature Rev. Immunol.* **8,** 9–21 (2008).
15. Nakajima, S., Roswit, W. T., Look, D. C. & Holtzman, M. J. A hierarchy for integrin expression and adhesiveness among T cell subsets that is linked to TCR gene usage and emphasizes V delta 1+ gamma delta T cell adherence and tissue retention. *J. Immunol.* **155,** 1117–1131 (1995).
16. Wesch, D. *et al.* Direct costimulatory effect of TLR3 ligand poly(I:C) on human γδ T lymphocytes. *J. Immunol.* **176,** 1348–1354 (2006).
17. Wilson, K. C., Center, D. M. & Cruikshank, W. W. The effect of interleukin-16 and its precursor on T lymphocyte activation and growth. *Growth Factors* **22,** 97–104 (2004).
18. Wesch, D., Peters, C., Oberg, H. H., Pietschmann, K. & Kabelitz, D. Modulation of gammadelta T cell responses by TLR ligands. *Cell. Mol. Life Sci.* **68,** 2357–2370 (2011).
19. Bajoghli, B. *et al.* A thymus candidate in lampreys. *Nature* **470,** 90–94 (2011).
20. Ariotti, S. *et al.* Tissue-resident memory $CD8^+$ T cells continuously patrol skin epithelia to quickly recognize local antigen. *Proc. Natl Acad. Sci. USA* **109,** 19739–19744 (2012).
21. Smith, J. J. *et al.* Sequencing of the sea lamprey (*Petromyzon marinus*) genome provides insights into vertebrate evolution. *Nature Genet.* **45,** 415–421 (2013).

Supplementary Information is available in the online version of the paper.

Acknowledgements We thank C. L. Turnbough Jr for providing *B. anthracis* exosporium, H. Yi for help with electron microscopy, S. A. Durham and R. E. Karaffa II for help with cell sorting, S. Holland for help with gene orthology analysis, Q. Han for help with cloning, and B. R. Herrin, M. Kasahara and Y. Sutoh for suggestions and discussion. M.H., P.G., N.M., S.D. and M.D.C. are supported by National Institutes of Health grants (R01AI072435 and R01GM100151) and the Georgia Research Alliance; M.S. and T.B. are supported by the Max Planck Society.

Author Contributions M.H., P.G., N.M., M.S., S.D., T.B. and M.D.C. designed the research, analysed data and wrote the paper; M.H., P.G., N.M., M.S., S.D. and T.B. carried out the research.

Author Information Sequence data have been deposited in GenBank/EMBL/DDBJ databases under accession numbers KF385949–KF385955. Reprints and permissions information is available at www.nature.com/reprints. The authors declare no competing financial interests. Readers are welcome to comment on the online version of the paper. Correspondence and requests for materials should be addressed to M.D.C. (max.cooper@emory.edu).

METHODS

Animals, antigens and mitogens. Two outbred species of lamprey larvae (*Petromyzon marinus* and *Lampetra planeri*) were captured in the wild and housed in sand-lined aquaria. *Bacillus anthracis* exosporium was provided by C. L. Turnbough Jr. Lampreys were immunized with 10 μg of *B. anthracis* exosporium. Animals were injected with 25 μg poly(I:C) (Sigma) or 25 μg phytohaemagglutinin (PHA-L, Sigma).

Production of anti-VLRC monoclonal antibodies. *VLRC* complementary DNA constructs[9] were cloned into a fusion vector to produce chimaeric proteins of the VLRC antigen-binding domain and stalk region fused to the constant region of human immunoglobulin-G1 (IgG1). Lymphocytes from mice immunized with the chimaeric proteins were used for hybridoma production, and supernatants were screened for antibody reactivity against recombinant VLRC. Monoclonal antibodies specific for VLRC were used together with anti-VLRA and -VLRB antibodies for characterizing and purifying VLR-expressing cells.

ELISA. ELISA (enzyme-linked immunosorbent assay) plates were coated with VLRA–IgG1-Fc[5] or VLRC–IgG1-Fc fusion proteins for 12 h at 4 °C and blocked with 1% BSA in PBS for 3 h at 37 °C. Hybridoma culture supernatants were added for 2 h at 37 °C. VLR reactivity of antibodies was detected using alkaline phosphatase-conjugated goat anti-mouse immunoglobulin antibodies (Southern Biotech), developed with phosphatase substrate (Sigma) and read at 405 nm (Versamax microplate reader, Molecular Devices).

Flow cytometric analysis and sorting of VLRA, VLRB and VLRC lymphocytes. Leukocyte isolation from blood and tissues and staining for flow cytometry proceeded as described[5]. In brief, leukocytes from blood and tissues were stained with anti-VLRA rabbit polyclonal serum (R110), anti-VLRB mouse monoclonal antibody (4C4) and biotinylated anti-VLRC mouse monoclonal antibodies (1B4, 3A5, 10A5, 11B5) and matched secondary reagents. Flow cytometric analysis was performed on a CyAn ADP (Dako) or Accuri C6 (BD Biosciences) flow cytometers. $VLRA^+$, $VLRB^+$, $VLRC^+$ and VLR triple-negative cells in the lymphocyte gate were sorted on BD FACS Aria II (BD Bioscience) for genomic and quantitative RT–PCR analysis. The purity of the sorted cells was 96.5 ± 1.5% ($VLRA^+$), 96.1 ± 1.4% ($VLRB^+$), 98.7 ± 1.3% ($VLRC^+$) and 97.9 ± 1.4% (triple-negative).

Immunofluorescence microscopy. Tissue samples were prepared and stained as described previously[19] using anti-VLRA rabbit serum (R110) and anti-VLRC monoclonal antibodies (3A5). Fluorescence microscopy was performed with a Zeiss Axiovert 200M and images were processed with Adobe Photoshop (Adobe Systems). For cell-number counts from intestinal epithelium and epidermis, the total numbers of positive cells from single 7-μm sections were counted for both tissues in a total of five larvae.

Proliferation assay. Lampreys stimulated with antigen, mitogen or poly(I:C) were injected with 5 μg of 5-ethynyl-2′-deoxyuridine (Invitrogen) in 40 μl 0.67 × PBS and returned to aquaculture for 24 h before collecting leukocytes for flow cytometry analysis as described[5].

Lymphocyte counts. Lymphocytes were prepared from lamprey blood and kidneys by passage through 70 μm cell strainers (BD Biosciences), producing single-cell suspensions. Cells were washed and resuspended in 1 ml 0.67 × PBS. Total cells were counted in 25 μl of each sample on an Accuri C6 flow cytometer. The total number of cells in the 'lymphocyte gate' was calculated by the formula: total lymphocyte number = number of cells in the lymphocyte gate × 40 (dilution factor). Lymphocytes were then stained with anti-VLRA, -VLRB and -VLRC antibodies to determine the percentages of $VLRA^+$, $VLRB^+$ and $VLRC^+$ cells, which were used to calculate the numbers of lymphocytes of each type.

VLR expression in transfected HEK-293T cells. *VLRB*- and *VLRC*-pIRESpuro2 plasmids were transfected into HEK-293T cells cultured in DMEM containing 5% FBS using linear polyethylenimine (PEI), MW 25,000 (Polysciences) at a 3:1 PEI:DNA ratio. Cells were separated from supernatants 48 h after transfection by centrifugation at 300*g* and lysed in 1% NP-40 lysis buffer.

Immunoblot analysis. Samples were separated on 11% non-reducing SDS–PAGE gels before transfer to polyvinylidene fluoride membranes (Millipore). Membranes were blocked overnight with 5% skimmed milk (US Biological) and incubated with anti-VLRB (4C4) or anti-VLRC (3A5) antibodies for 1 h. After five washes with 0.5% Tween-20 in 1× PBS, membranes were incubated with horseradish peroxidase (HRP)-conjugated goat anti-mouse immunoglobulin polyclonal antibodies (Dako) and washed. Blots were developed using SuperSignal West Pico Chemiluminescent substrate (Thermo Scientific).

Genomic PCR. Genomic DNA was extracted from $VLRA^+$, $VLRB^+$, $VLRC^+$ and VLR triple-negative-sorted lymphocytes using DNeasy kit (QIAGEN). Genomic PCR was carried out using primers VLRA-F and VLRA-R, VLRB-F and VLRB-R or VLRC-F and VLRC-R (Expand Long Template, Roche). Primers are listed in Supplementary Table 1.

RT–PCR. Total RNA was extracted from sorted cells of lamprey blood and tissues (kidneys, typhlosole, gill and skin) and reverse-transcribed using random hexamers (Invitrogen). KOD Hot Start DNA Polymerase (TOYOBO) and Ex Taq were used to amplify the *VLR* genes. When necessary, the PCR products were cloned into pBluescript (Stratagene) or pCR4-TOPO (Invitrogen) vector and sequenced. Primers used for PCR are listed in Supplementary Table 1.

***VLRC* assemblies from *Lampetra planeri*.** Genomic DNA was procured from the thymoid region of gill filaments of *Lampetra planeri* larvae by laser-capture micro-dissection, essentially as described[19]. *VLRC* genes were amplified using high-fidelity Phusion Taq polymerase (Invitrogen) and primers VLRC5.1 and VLRC3 (Supplementary Table1), cloned into the pGEM-T vector (Promega) and sequenced; in some cases, sequences were cloned after a second amplification step using primers VLRC5.2 and VLRC3. Non-functional sequences exhibited either internal stop codons, frame-shift mutations, or consisted of partial assemblies.

RNA *in situ* hybridization analyses. RNA *in situ* hybridization analyses were performed on paraffin-embedded tissue sections of *L. planeri* larvae, essentially as described[19]. The *CDA1* probe has been described previously[19].

Quantitative real-time PCR. Target gene sequences were obtained from the lamprey genome database[21] and subsequent *in silico* analysis (including phylogenetic analysis) was performed as described previously[9]. RNA was extracted from each population using RNeasy kits with on-column DNA digestion by DNase I (QIAGEN). First-strand cDNA was synthesized with random hexamer primers and Superscript III (Invitrogen). Quantitative real-time PCR was carried out with SYBR Green on a 7900HT ABI Prism (Applied Biosystems). Quantitative real-time PCR reactions were performed to evaluate the expression of each gene orthologue. Five separate determinations were carried out for heat-map analysis. The value of the target gene expression was normalized to β-actin. The normalized value for each gene was compiled into a heat map (*z*-scores) with three-colour scale. Red, $z = 1.5$; blue, $z = -1.5$; white, $z = 0$ (z = (each value − average)/standard deviation). Primers and the values of the target gene are described in Supplementary Tables 1 and 2, respectively.

Electron microscopy. Tissue lymphocytes from naive or PHA-stimulated lamprey larvae were sorted on a BD FACS Aria II (BD Biosciences). The VLRC-positive cells were prepared for transmission electron microscopic analysis as described previously[5].

Statistical analysis. Statistical significance was determined by a two-sample Student's *t*-test and Fisher's exact test.